IEEE Photonics Journal
An IEEE Photonics Society Publication

1.3 to 1.55 μm All-Optical Wavelength Conversion for VCSEL-to-VCSEL Inversion and Logic

Volume 4, Number 3, June 2012

Simone Mazzucato
Kevin Schires
Antonio Hurtado
Michael J. Adams
Ian D. Henning
Naci Balkan

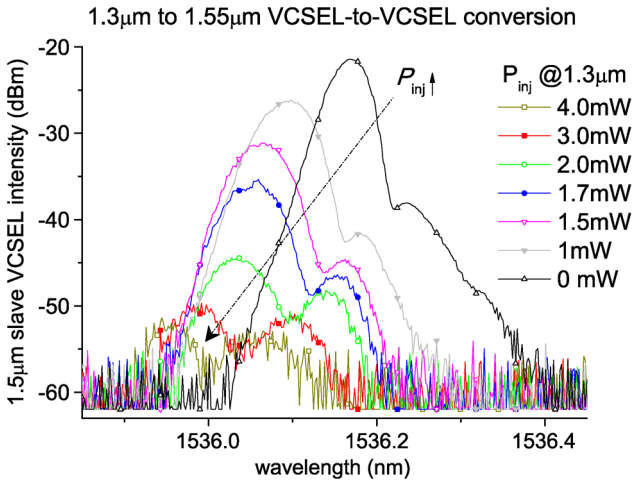

DOI: 10.1109/JPHOT.2012.2198803
1943-0655/$31.00 ©2012 IEEE

1.3 to 1.55 μm All-Optical Wavelength Conversion for VCSEL-to-VCSEL Inversion and Logic

Simone Mazzucato, Kevin Schires, Antonio Hurtado, Michael J. Adams, Ian D. Henning, and Naci Balkan

School of Computer Science and Electronic Engineering, University of Essex, CO4 3SQ Colchester, U.K.

DOI: 10.1109/JPHOT.2012.2198803
1943-0655/$31.00 ©2012 IEEE

Manuscript received March 22, 2012; revised May 1, 2012; accepted May 1, 2012. Date of current version May 22, 2012. This work was supported by the U.K. EPSRC under Grant EP/G023972/1 and the European Commission under the Marie Curie Fellowships program Grant PIOF-GA-2010-273822, as well as COST Action MP0805. Corresponding author: S. Mazzucato (e-mail: smazzu@essex.ac.uk).

Abstract: We demonstrate all-optical wavelength conversion from the O to the C band using a 1550-nm commercial vertical-cavity surface-emitting laser (VCSEL) subject to external optical injection at 1300 nm. For the first time to our knowledge, we show that this configuration can also be used to develop all-optical inverters and cross-band NAND and NOR gates based on VCSEL devices, and investigate their potential speed of operation.

Index Terms: Optical wavelength conversion, switching converters, vertical cavity surface emitting lasers.

1. Introduction

All-optical signal processing has become a key feature in communication systems, as it reduces the number of intermediate electrical stages used to process and enhance the optical signals, leading to a reduction in the system complexity and total cost [1]. When considering the transmitter-receiver link, a proper choice in the type of devices used is essential. In this sense, vertical-cavity surface-emitting lasers (VCSELs) have important competitive advantages to commonly used edge-emitting lasers, due to their higher performance in terms of temperature stability, fiber-coupling efficiency, lower threshold current and power consumption, and low cost in fabrication, testing and packaging [2]. Therefore, low-cost solutions for signal processing using VCSELs form an area of increased research activity, and have already been demonstrated for different purposes including for example AM to FM conversion [3], up-conversion [4] and optical buffering [5]. These signal processing applications are of particular interest as directly performed by the same type of laser sources used in the transmission link. Although low-cost ways of performing wavelength conversion have been investigated, these solutions generally rely on the addition to the setup of an extra active component, usually an optical amplifier [6], [7]. In this paper, we propose a novel way of converting optical data at 1.3 μm to 1.5 μm using a commercially available C-band VCSEL. In addition to cross-band wavelength conversion, all-optical inversion operation is also obtained. We further experimentally demonstrate cross-band wavelength conversion and inversion using a VCSEL-to-VCSEL optical injection configuration.

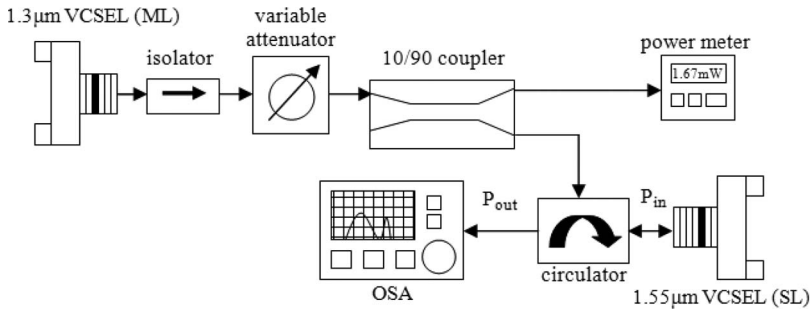

Fig. 1. Experimental setup to pump 1.55 μm VCSEL with 1.3 μm VCSEL.

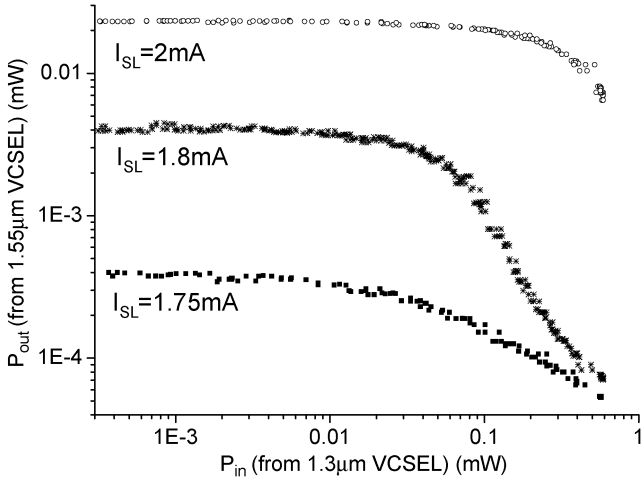

Fig. 2. P_{out} versus P_{in} curve at various SL driving current.

2. Experimental Results and Discussion

Fig. 1 presents the experimental setup used to demonstrate cross-band wavelength conversion from the O- to the C-band. Two commercially available VCSELs (Raycan [8]) were used. Light from a 1330 nm-VCSEL (master laser, ML) was injected into a 1536 nm-VCSEL (slave laser, SL) with threshold current I_{th} of 1.75 mA at $T = 20\ ^{\circ}C$.

The 1330 nm-VCSEL ML was driven well above threshold and its optical power was first controlled with a variable attenuator and split in two using a 90/10 coupler. The 10% output was used to monitor the optical input power whereas the 90% output was injected into the SL (P_{in}) *via* an optical circulator. The light of the SL was analyzed with an optical spectrum analyzer (OSA). We refer to the peak power of the optical spectrum as P_{out}. Fig. 2 presents the evolution of P_{out} versus P_{in} for few SL bias currents I_{SL}. The SL output is significantly suppressed by the ML injected light when the SL is biased close to threshold. On the other hand, a small reduction of P_{out} was observed for SL bias currents further above I_{th}, due to the limited maximum optical power emitted by the ML (max $P_{in} = 0.75$ mW).

Since these results demonstrate the possibility to control the 1.55 μm VCSEL emission with the 1.3 μm input, in order to achieve a significant suppression of the SL emitted light for currents well above I_{th}, a 1.3 μm emitting tunable laser (TL) with a maximum output power of 6 mW was used as ML instead of the 1330 nm-VCSEL. Fig. 3 shows the evolution of the SL spectra when changing the injected power (at fixed $I_{SL} > I_{th}$) [Fig. 3(a)] and when changing the driving current without optical injection [Fig. 3(b)]. Similar trends are observed increasing P_{in} or decreasing I_{SL}. Fig. 4 summarizes what observed in Fig. 3, showing the SL peak amplitude versus peak wavelength for

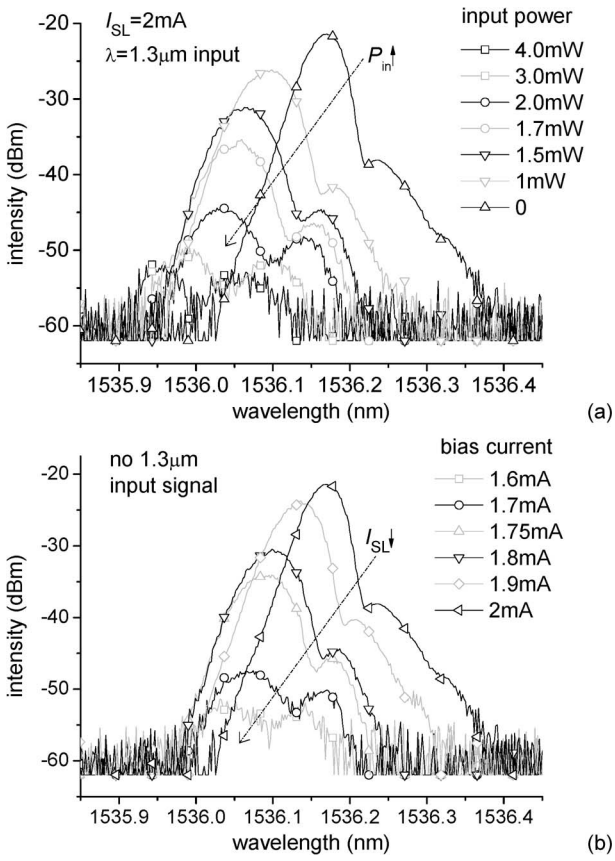

Fig. 3. 1.55 μm spectra taken at different input power (a), and different driving current (b). The dotted arrows visually indicate the evolution of the spectra as function of increasing power and decreasing current.

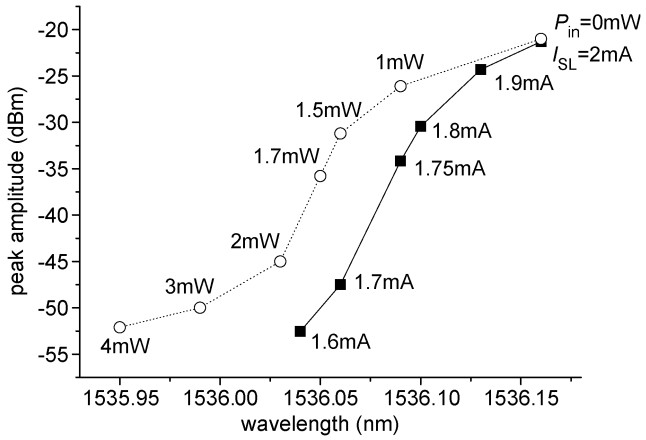

Fig. 4. Evolution of the 1.55 μm SL peak amplitude versus wavelength trend at different bias current and incident power, as obtained from the analysis of Fig. 3.

different values of externally injected optical power P_{in} and different currents. It is clear that, in addition to a decrease in intensity (even reaching complete mode suppression), the peak wavelength also experiences a blue-shift with increasing P_{in} For fixed SL bias current, the rate of this shift in wavelength was 0.05 nm/mW or 6 GHz/mW, and was found to be independent of I_{SL}.

We have also explored the effect of optical injection at different wavelengths from 1265 to 1345 nm (wavelength range of the TL). The suppression in the light emitted by the slave VCSEL with external injection did not change for different injection wavelengths. This factor might be of particular interest for potential device designs unaffected by wavelength shifts and detuning effects.

The observed wavelength shift can provide some details on the mechanisms behind the suppression of the SL emission by the ML's injected light. The 1.3 μm optical injection affects the SL behavior through heating and carrier injection. Local internal heating effects due to absorption by the device layers can play a significant role in the VCSEL emission, as described in [9] and [10].

The effect of increased carrier injection into the SL results in the observed blue-shift of the VCSEL's emission wavelength, which is due to the reduction of the device effective refractive index [11] and the shift in the material gain. In general, a change in the injected photon density results in carrier density changes. The consequent changes in the material refractive index lead therefore to shifts in the cavity mode frequency and the shift in the gain spectrum [12]. This variation of the internal carrier density due to the increase of P_{in} has an effect rather similar to a decrease of the current I_{SL}, as also plotted in Fig. 3, or, more precisely, to an increase of the SL threshold current I_{th}. It was observed that the SL threshold current grows with optical injection. It is true that an increase in I_{th} could be explained by considering only thermal effects. However, investigation of the SL threshold current and corresponding wavelength peak λ_{th} (i.e., the emission wavelength of SL when driven at $I = I_{th}$) showed that thermal effects are not sufficient to account for the observed variations in current and wavelength. These shifts are presented in Fig. 5(a) and (b), respectively. The plotted data are taken by analyzing the light-current curves and spectra when changing the temperature or the injected power. Without optical injection, the SL threshold current grows with temperature in a parabolic-like trend, with a total change over 35 °C of about 5 mA, while λ_{th} grows linearly at around 0.2 nm/°C. In presence of injection, at $T = 20$ °C, the increase for I_{th} is of 4 mA in 4 mW change, while λ_{th} increase of about 0.3 nm/mW.

In Fig. 5(a) the SL threshold current is plotted as function of T and P_{in}, where the x-axes have been scaled to try overlapping the two curves. Observing Fig. 5(a) only, a linear relation between photon injection and lattice temperature could be speculated. When increasing either the temperature or the injected power, I_{th} in the SL increases roughly in the same way. However, plotting λ_{th} for the SL versus T and P_{in} using the same x-scale ranges of Fig. 5(a) shows that the two effects are highly different. This is shown in Fig. 5(b). Moreover, from the inset of the same figure it is evident how $I - L$ curves taken at $P_{in} = 4$ mW at $T = 20$ °C and at $T = 55$ °C without injection greatly diverge, enforcing the conclusion that the heating effect alone cannot explain the SL signal change with optical pump. For a clearer insight and understanding, it would be desirable to repeat this experiment using injection of short optical pulses (and/or short pulse current modulation) [13], so that thermal contributions are expected to reduce considerably.

Figs. 2–4 clearly show that the ML's injection can change the SL's output power and also shift its emission wavelength; hence an application of this result could be through the modulation of the ML power, resulting in modulation of SL power and wavelength, so that the device could be used for coarse and fine frequency (wavelength) conversion.

Therefore, having demonstrated the influence of 1.3 μm injection into the 1.55 μm VCSEL, a first application of this cross-band master-slave configuration could be the development of a novel switch system suitable for use in telecomm networks as converter between optical links operating in the O and C bands. Additionally this proposed configuration could be used to create optical logical gates. For instance, we could set the power of a 1.3 μm master VCSEL with a value sufficiently high to suppress the solitary emission of a 1550 nm slave VCSEL (HIGH state, or "1"). This turns the emission of the slave VCSEL from its solitary state (HIGH) to a suppressed state (LOW output state, or 0"). Returning the ML power to zero or to a level insufficient to affect the SL emission (LOW) then puts the SL back in its HIGH state. As a result of this process an inverted copy of the injected signal at 1330 nm is obtained at the output of the 1550 nm-VCSEL. Such behavior shows similarities to the all-optical inversion presented by Quirce *et al.* [14] but in this work we present for the first time the potential of a VCSEL-to-VCSEL optical injection configuration for the development of cross-band all-optical inverters with input and output in the O and C band, respectively.

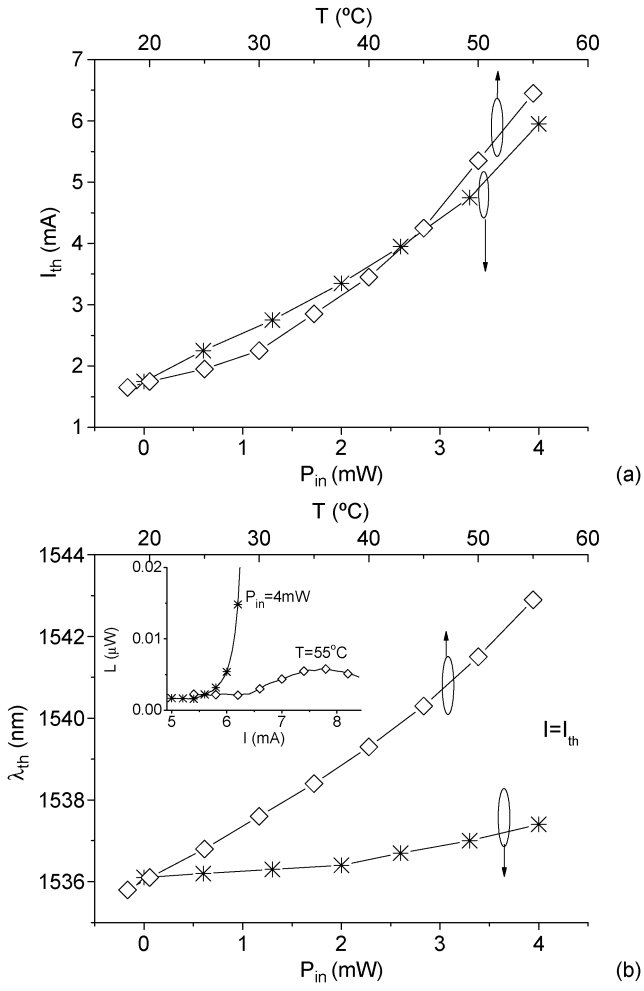

Fig. 5. Changes in the (a) threshold current and (b) threshold wavelength emission of SL laser under the influence of temperature and photon injection. The inset shows the different current-light $(I - L)$ curves obtained at $P_{in} = 4$ mW at 20 °C and without optical injection at $T = 55$ °C.

The use of several MLs can allow the creation of a series of 1.3-to-1.55 μm cross-band all-optical logic gates. For this purpose the setup of Fig. 1 was modified to replace the single ML with two similar 1.3 μm VCSELs combined *via* a 50/50 coupler. This modified setup was used to create a NAND or a NOR logic gate. These gates are of particular interest as any other type of logic operation can be derived from combinations of them.

The inset of Fig. 6 shows the results when arranging the system for a NAND gate operation. A threshold power P_T is chosen at the output gate to distinguish between the LOW and HIGH states at the gate's output. This value is chosen in such a way that the slave VCSEL's output is LOW only when both MLs are set at their HIGH inputs. This NAND gate can be changed into a NOR gate operation by either simply setting P_T to a higher value or using different operating conditions for the MLs (higher pump power for instance) or the SL (i.e., lower bias current). Fig. 6 presents a graph of P_{out} against P_{in} that allows the identification of the value of P_T to be chosen in order to create this NOR gate.

To study the speed of the proposed system, we investigated the dynamic behavior of the inverter SL under optical injection of light from two tunable lasers; the frequency difference between the injected lasers was used to measure the frequency response of the gate via photomixing in the VCSEL [15]. Fig. 7 presents the setup used for this configuration. A second 1.3 μm TL was coupled with the previously used one *via* a 90/10 coupler, and their polarization and power were controlled

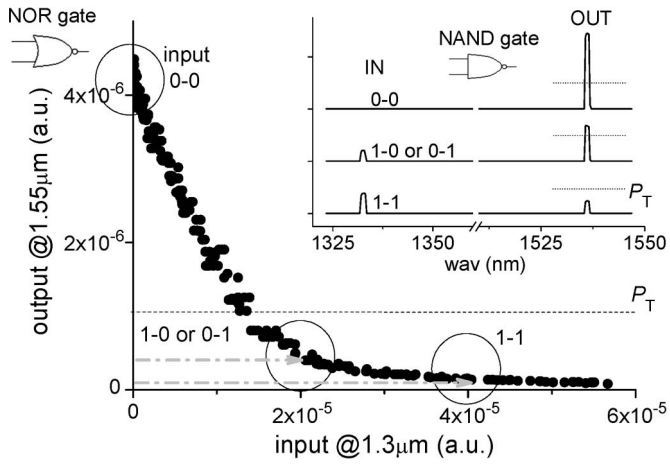

Fig. 6. NOR (main figure) and NAND (inset) gate results.

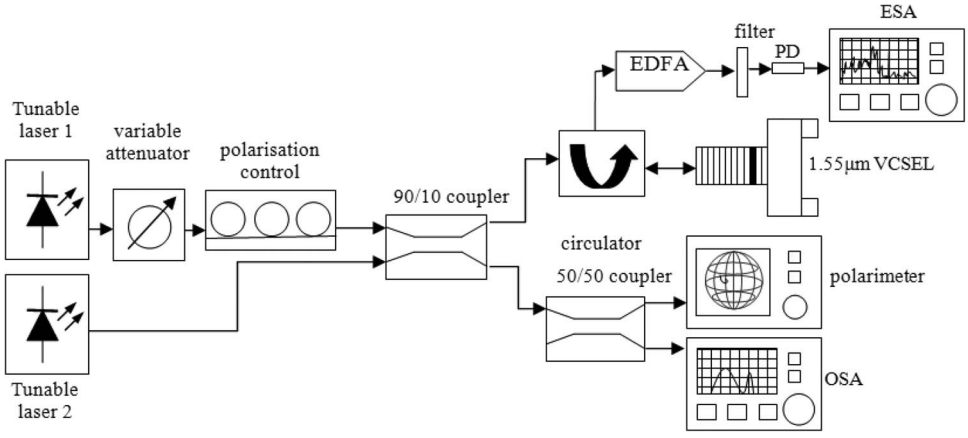

Fig. 7. Setup for RF bandwidth measurement of the logical gates. PD: photodiode, ESA: Electrical Spectrum Analyzer.

to be identical to each other. The 10% output of the coupler was used to monitor simultaneously the polarization, power and wavelength of both lasers. The 90% output was injected into the SL *via* an optical circulator and the output of the SL was analyzed with a radio frequency (RF) spectrum analyzer. An Er-doped fiber amplifier (EDFA) was placed after the circulator in order to both amplify the light of the SL and attenuate the light from the two MLs (at 1.3 μm). A bandpass filter centered on the SL was also placed between the EDFA and the spectrum analyzer in order to suppress the EDFA's amplified spontaneous emission and to further attenuate the unwanted light contribution from the MLs.

By changing the wavelength of one of the two TLs and ensuring that the powers and polarizations of both MLs were equal and constant ($P_{in} \sim 2$ mW at the SL), beatings of equal modulation depth and frequencies between DC and 3 GHz were produced at the SL. The RF spectrum of the SL was measured for several beating frequencies within this range and for SL bias currents between 2 and 3 mA.

These spectra were then combined to represent the frequency response of the VCSEL and measure its 3 dB bandwidth. Fig. 8 presents the measurements of the relaxation oscillation frequency (ROF) and the bandwidth as a function of the square root of the overdrive $(I - I_{th})$ of the VCSEL [12]. The results show the linear dependence on overdrive (or equivalently, output power [15]) expected for measurements of frequency response by photomixing. For the ROF

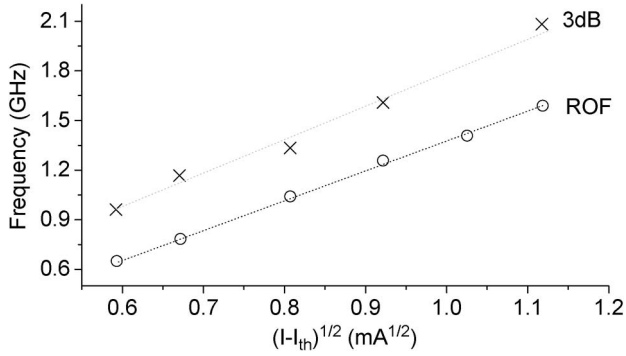

Fig. 8. ROF and 3 dB bandwidth data of the logic gate for different bias.

measurement, we used measurements of the RF spectrum to find the frequency of the bump in the VCSEL relative intensity noise. On average, the bandwidth of the gate was found to be 1.4 times the ROF of the VCSEL. Since the ML used is only rated at 2.5 Gb/s, we expect that devices with higher ROF values will allow the demonstration of even faster cross-band logic gates.

3. Conclusion

We have made a first demonstration of all-optical wavelength conversion and inverting operation at 1550 nm with a VCSEL subject to external optical injection at 1.3 μm. Full-suppression of the emission mode and a blue-shift in peak wavelength for the SL were both observed by controlling the injected power. Starting from this observation, inverter function and hence NAND and NOR basic logic gate operation was demonstrated.

A modulation bandwidth measurement has been performed to provide an estimation of the maximum operating speed that could be obtained for the 1.3–1.55 μm wavelength conversion and logic applications described here. The results, which were found to be limited by the inherent ROF of the employed devices, show that GHz operation could be attained. However, further studies would be needed to determine not only the speed but the magnitudes of extinction ratio and fan-out of the applications described in this work.

References

[1] O. Wada, "Recent progress in semiconductor-based photonic signal-processing devices," *IEEE J. Sel. Topics Quantum Electron.*, vol. 17, no. 2, pp. 309–319, Mar./Apr. 2011.
[2] S. F. Yu, *Analysis and Design of Vertical Cavity Surface Emitting Lasers*. New York: Wiley, 2003.
[3] J. Kitching, S. Knappe, N. Vukicevic, L. Hollberg, R. Wynands, and W. Weidmann, "A microwave frequency reference based on VCSEL-driven dark line resonances in Cs vapor," *IEEE Trans. Instrum. Meas.*, vol. 49, no. 6, pp. 1313–1317, Dec. 2000.
[4] S. B. Constant, Y. Le Guennec, G. Maury, N. Corrao, and B. Cabon, "Low-cost all-optical up-conversion of digital radio signals using a directly modulated 1550-nm emitting VCSEL," *IEEE Photon. Technol. Lett.*, vol. 20, no. 2, pp. 120–122, Jan. 2008.
[5] H. Kawaguchi, T. Mori, Y. Sato, and Y. Yamayoshi, "Optical buffer memory using polarization bistable vertical-cavity surface-emitting lasers," *Jpn. J. Appl. Phys.*, vol. 45, no. 33–36, pp. L894–L897, Aug. 2006.
[6] D. N. Maywar, Y. Nakano, and G. P. Agrawal, "1.31-to-1.55μm wavelength conversion by optically pumping a distributed feedback amplifier," *IEEE Photon. Technol. Lett.*, vol. 12, no. 7, pp. 858–860, Jul. 2000.
[7] P. E. Barnsley and P. J. Chidgey, "All-optical wavelength switching from 1.3μm to a 1.55μm WDM wavelength routed network: System results," *IEEE Photon. Technol. Lett.*, vol. 4, no. 1, pp. 91–94, Jan. 1992.
[8] M. R. Park, O. K. Kwon, W. S. Han, K. H. Lee, S. J. Park, and B. S. Yoo, "All-epitaxial InAlGaAs-InP VCSELs in the 1.3–1.6-μm wavelength range for CWDM band applications," *IEEE Photon. Technol. Lett.*, vol. 18, no. 16, pp. 1717–1719, Aug. 2006.
[9] B. Tell, F. Brown-Goebeler, R. E. Leibenguth, F. M. Baez, and Y. H. Lee, "Temperature dependence of GaAs-AlGaAs vertical cavity surface emitting lasers," *Appl. Phys. Lett.*, vol. 60, no. 6, pp. 683–685, Feb. 1992.
[10] C. Chen, P. Leisher, A. Allerman, K. Geib, and K. Choquette, "Temperature analysis of threshold current in infrared vertical-cavity surface emitting lasers," *IEEE J. Quantum Electron.*, vol. 42, no. 10, pp. 1078–1083, Oct. 2006.
[11] B. R. Bennett, R. A. Soref, and J. A. Del Alamo, "Carrier-induced change in refractive index of InP, GaAs, and InGaAsP," *IEEE J. Quantum Electron.*, vol. 26, no. 1, pp. 113–122, Jan. 1990.

[12] L. A. Coldren and S. W. Corzine, *Diode Lasers and Photonic Integrated Circuits*. Hoboken, NJ: Wiley, 1995.
[13] Y. Hong, C. Masoller, M. S. Torre, S. Priyadarshi, A. A. Qader, P. S. Spencer, and K. A. Shore, "Thermal effects and dynamical hysteresis in the turn-on and turn-off of vertical-cavity surface-emitting lasers," *Opt. Lett.*, vol. 35, no. 21, pp. 3688–3690, Nov. 2010.
[14] A. Quirce, J. R. Cuesta, A. Hurtado, K. Schires, A. Valle, L. Pesquera, I. Henning, and M. J. Adams, "Dynamic characteristics of an all-optical inverter based on polarization switching in long-wavelength VCSELs," *IEEE J. Quantum Electron.*, vol. 48, no. 5, pp. 588–595, May 2012.
[15] K. J. Vahala and M. A. Newkirk, "Parasitic-free modulation of semiconductor lasers," *IEEE J. Quantum Electron.*, vol. QE-25, no. 6, pp. 1393–1398, Jun. 1989.